Journal of Experimental Botany, Vol. 61, No. 9, pp. 2479–2490, 2010
doi:10.1093/jxb/erq093 Advance Access publication 21 April, 2010
This paper is available online free of all access charges (see http://jxb.oxfordjournals.org/open_access.html for further details)

Journal of Experimental Botany
www.jxb.oxfordjournals.org

RESEARCH PAPER

Phenotypic plasticity in cell walls of maize *brown midrib* mutants is limited by lignin composition

Wilfred Vermerris[1,2,3,*], Debra M. Sherman[4] and Lauren M. McIntyre[1,5]

[1] University of Florida Genetics Institute, Gainesville, FL 32610, USA
[2] Agronomy Department, University of Florida, Gainesville, FL 32610, USA
[3] Department of Agricultural and Biological Engineering, Purdue University, West Lafayette, IN 47907, USA
[4] Department of Horticulture and Landscape Architecture, Purdue University, West Lafayette, IN 47907, USA
[5] Department of Molecular Genetics and Microbiology, University of Florida, Gainesville, FL 32610, USA

* To whom correspondence should be addressed: E-mail: wev@ufl.edu

Received 4 February 2010; Accepted 10 March 2010

Abstract

The hydrophobic cell wall polymer lignin is deposited in specialized cells to make them impermeable to water and prevent cell collapse as negative pressure or gravitational force is exerted. The variation in lignin subunit composition that exists among different species, and among different tissues within the same species suggests that lignin subunit composition varies depending on its precise function. In order to gain a better understanding of the relationship between lignin subunit composition and the physico-chemical properties of lignified tissues, detailed analyses were performed of near-isogenic *brown midrib2* (*bm2*), *bm4*, *bm2-bm4*, and *bm1-bm2-bm4* mutants of maize. This investigation was motivated by the fact that the *bm2-bm4* double mutant is substantially shorter, displays drought symptoms even when well watered, and will often not develop reproductive organs, whereas the phenotypes of the individual *bm* single mutants and double mutant combinations other than *bm2-bm4* are only subtly different from the wild-type control. Detailed cell wall compositional analyses revealed midrib-specific reductions in Klason lignin content in the *bm2*, *bm4*, and *bm2-bm4* mutants relative to the wild-type control, with reductions in both guaiacyl (G)- and syringyl (S)-residues. The cellulose content was not different, but the reduction in lignin content was compensated by an increase in hemicellulosic polysaccharides. Linear discriminant analysis performed on the compositional data indicated that the *bm2* and *bm4* mutations act independently of each other on common cell wall biosynthetic steps. After quantitative analysis of scanning electron micrographs of midrib sections, the variation in chemical composition of the cell walls was shown to be correlated with the thickness of the sclerenchyma cell walls, but not with xylem vessel surface area. The *bm2-bm4* double mutant represents the limit of phenotypic plasticity in cell wall composition, as the *bm1-bm2-bm4* and *bm2-bm3-bm4* mutants did not develop into mature plants, unlike the triple mutants *bm1-bm2-bm3* and *bm1-bm3-bm4*.

Key words: *brown midrib*, cell wall, lignin, maize, SEM, *Zea mays*.

Introduction

The chemical composition and physical properties of materials are intricately associated. In the case of polymers, the nature of the monomer(s), parameters such as the degree of crosslinking, and the average chain length determine physical properties such as elasticity, glass transition temperature, and thermostability. This applies both to synthetic polymers (Bicerano, 2002), and biological polymers such as starch (Kortstee *et al.*, 1998; Groth *et al.*, 2008) and pectins (Willats *et al.*, 2001).

The cell wall polymer lignin is a complex aromatic polymer present in the cell walls of plants, in particular, secondary cell walls of the xylem and sclerenchyma. Lignin provides structural support and facilitates water transport and is also important in the defence against pests and

© 2010 The Author(s).
This is an Open Access article distributed under the terms of the Creative Commons Attribution Non-Commercial License (http://creativecommons.org/licenses/by-nc/2.5), which permits unrestricted non-commercial use, distribution, and reproduction in any medium, provided the original work is properly cited.

pathogens. Lignin is formed via the oxidative coupling of monolignols, synthesized via the shikimic acid and phenylpropanoid pathways (reviewed by Boerjan *et al.*, 2003; Ralph *et al.*, 2004). The three main monolignols in maize and other grasses are *p*-coumaryl alcohol, coniferyl alcohol, and sinapyl alcohol, which give rise to *p*-hydroxyphenyl (H), guaiacyl (G), and syringyl (S) residues, respectively.

In the cell walls of grasses such as maize, lignin is chemically cross-linked with glucuronoarabinoxylans (GAXs) via ferulate and diferulate bridges (Ralph *et al.*, 1995; Hatfield *et al.*, 1998; Zhang *et al.*, 2009). The GAXs in turn are associated with cellulose microfibrils through hydrogen bonding and Van der Waals forces, resulting in a complex matrix (Carpita and Gibeaut, 1993).

There is considerable variation in lignin subunit composition between species, between tissues within the same species, and between different developmental stages (Terashima *et al.*, 1993; Müsel *et al.*, 1997; Joseleau and Ruel, 1997; Vermerris and Boon, 2001), which is possibly a reflection of different demands placed on lignified tissues (Boyce *et al.*, 2004). The plant must somehow be able to control this spatio-temporal variation in lignin composition, but the precise mechanism is unclear. Chemical control has been proposed, whereby the composition of the surrounding matrix affects the reaction kinetics (Hatfield and Vermerris, 2001). An opposing view is biological control, which would require the involvement of proteins that stipulate the formation of the different interunit linkages (Davin and Lewis, 2005; Davin *et al.*, 2008).

Regardless of the mechanism the plant employs to establish a certain lignin subunit composition, the physical properties of the lignified cell wall, including wall strength and water conductivity, ultimately depend on the chemical composition. Defining the relationship between structure and function of cell wall components is important for understanding the evolution of land plants and plays a key role in the development of new crops with cell wall properties that are more amenable to down-stream applications, such as the production of green chemical feedstocks (Yang and Wyman, 2004; Vermerris *et al.*, 2007; Saballos *et al.*, 2008).

Variation in lignin subunit composition can be introduced through the use of mutations in lignin biosynthetic genes or through transgenic down-regulation of gene expression (Boerjan *et al.*, 2003; Vanholme *et al.*, 2008). A group of cell wall mutants in maize is known as the *brown midrib* (*bm*) mutants. These mutants, *bm1*, *bm2*, *bm3*, and *bm4*, have reddish-brown vascular tissue in the leaves and stems as a result of changes in cell wall composition. The *bm1* mutant has reduced activity of the lignin biosynthetic enzyme cinnamyl alcohol dehydrogenase (CAD) (Halpin *et al.*, 1998). Consequently, the cell walls of this mutant contain increased levels of cinnamaldehydes (Halpin *et al.*, 1998; Marita *et al.*, 2003). The *bm1* mutation is unlikely to be in the *CAD* gene itself (Guillaumie *et al.*, 2007*a*) and the function of *Bm1* remains to be elucidated, as is the case for *Bm2* and *Bm4*. The *bm2* mutant contains fewer guaiacyl residues (Chabbert *et al.*, 1994*b*) and has a disturbance in the tissue-specific patterns of lignification (Vermerris and Boon, 2001). NMR analyses of lignin isolated from *bm4* stems harvested just before anthesis did not reveal major changes relative to the wild-type control (Marita *et al.*, 2003). The *Bm3* gene encodes the enzyme caffeic acid *O*-methyl transferase (Vignols *et al.*, 1995; Morrow *et al.*, 1997). Mutations in this gene result in lignin with a higher G/S ratio and the incorporation of 5-hydroxyconiferyl alcohol (Lapierre *et al.*, 1988; Chabbert *et al.*, 1994*a*), which can form benzodioxane structures (Marita *et al.*, 2003).

Phenotyping and chemical and structural analyses on the *bm2*, *bm4*, and *bm2-bm4* mutants were performed to gain a better understanding of how changes in lignin subunit composition affect plant development, possibly through changes in the ultrastructure of the conductive and supportive tissues (Nakashima *et al.*, 2008). From these analyses it is apparent that lignin subunit composition can vary considerably without affecting the overall performance of the maize plant, but that once a certain threshold is crossed, the plant is no longer able to develop and function normally.

Materials and methods

Plant material

The development of the *bm1*, *bm2*, *bm4*, and *bm1-bm2* near-isogenic lines (NILs) in inbred line A619 following a minimum of six backcrosses has been described by Vermerris and McIntyre (1999). The *bm2–bm4* double mutant was created by crossing a *bm2* and a *bm4* NIL. The F_1 progeny was self-pollinated and putative double mutants were identified in the F_2 population, self-pollinated, and subjected to test crosses to both *bm2* and *bm4* single mutants to confirm the presence of the two mutations. The same approach was used to create the remaining three possible *bm* double mutant NILs: *bm1-bm3*, *bm2-bm3*, and *bm3-bm4*. The fact that these different mutant lines are all in the same genetic background makes it possible to attribute any phenotypic differences directly to the mutations.

The *bm1-bm2-bm4* triple mutant was generated by crossing *bm1-bm2* with *bm2-bm4*, followed by self-pollination of the F_1 progeny. Since both parents were homozygous for *bm2*, the F_2 progeny was homozygous for *bm2*, but segregating for *bm1* and *bm4*. Sixty seeds from each of three F_2 families were planted. Based on the reduced height of the *bm2-bm4* double mutant and normal height of the *bm1-bm4* double mutant, DNA from all small plants plus wild-type and *bm1* controls was isolated using the Plant Red ExtractNAmp kit (Sigma, St Louis, MO), and used to determine the genotype for the dupSSR10 simple sequence repeat marker, which is tightly linked to the *bm1* locus (www.maizegdb.org). The PCR was based on the manufacturer's instructions, and was performed in a 15 µl volume containing 50 ng of each primer (forward 5′-AGA AAA TGG TGA GGC AGG-3′, reverse 5′-TAT GAA ATC TGC ATC TAG AAA TTG-3′) using a three-step program consisting of an initial denaturation of 2 min at 94 °C, followed by 35 cycles of 10 s at 94 °C, 20 s at 55 °C and 40 s at 72 °C. PCR products were separated on a 4% SFR agarose gel (Amresco) containing ethidium bromide.

The triple mutants *bm1-bm2-bm3* and *bm1-bm3-bm4* were generated by crossing confirmed *bm1-bm2* and *bm2-bm3* double mutants, self-pollinating the F_1 progeny and selection in the F_2 progeny for triple mutants based on the molecular marker dup10SSR (see above) and a PCR-based detection of the *bm3-ref* allele (Vignols *et al.*, 1995) based on the presence of the B5

retrotransposon using the primers B5-29 (5′-GTT CTC TTC CTC GCC TTC CTC AG-3′) and *bm3*-L1522 (5′-ACG GGA TGA CGG CGT TCG AGT A-3′; Vermerris and Bout, 2003) using a three-step PCR program as described above with an annealing temperature of 64 °C. The genotype of the putative triple mutants was then confirmed by testcrosses to the individual single *bm* mutants. The *bm1-bm3-bm4* triple mutant was generated similarly after crossing *bm1-bm4* and *bm3-bm4*. Attempts to generate a *bm2-bm3-bm4* triple mutant by crossing *bm2-bm4* with *bm3-bm4* and by crossing *bm2-bm4* with *bm2-bm3* did not result in viable triple mutant plants.

Single and available double *bm* mutants along with the wild-type inbred line A619 were planted in the field in 5 m rows, spaced 0.76 m apart using a randomized complete block design with two replicates of 12 plants of each genotype. The field was located at the Agronomy Center for Research and Education near West Lafayette, IN. Plant height at anthesis was recorded for all plants. In addition, from each replicate three randomly selected plants wild-type, *bm2*, *bm4*, and *bm2-bm4* plants were sampled for chemical and ultrastructural analyses. The same field design was used the following year in a nearby field at the same location, with additional double mutants that had become available.

Scanning electron microscopy

Leaf six (the ear leaf) was harvested from wild-type, *bm2*, *bm4*, and *bm2-bm4* plants in the field after anthesis. The leaves were placed in water, and transported to the laboratory for fixation. A 1.5 cm strip containing the midrib was cut from each of the leaves at approximately 4 cm from the base of the leaf blade. The strips were immersed in primary fixative (4% glutaraldehyde in 0.1 M potassium phosphate buffer, pH 6.8) and cut into 2 mm sections. The sections were fixed overnight and then washed four times in buffer. The samples were subsequently fixed in 2% (w/v) OsO_4 in 0.1 M potassium phosphate buffer, pH 6.8, for 4 h followed by buffer and water washes (2× each). They were dehydrated in an ethanol series, critical-point dried (LADD Research Ind., Williston, VT), mounted, and sputter coated with AuPd prior to imaging.

Digital SEM images of two sections from each of the four genotypes were acquired using a JEOL JSM-840 scanning electron microscope (JEOL USA, Inc., Peabody, MA) operating at 5 kV. An overview image was generated for each sample at a magnification of ×200. Close-up images of the individual xylem vessels and sclerenchyma walls were generated at magnifications of ×750 and ×1000, respectively. Magnifications were calibrated using a carbon replica grid having line spacings of 0.463 μm.

Image analysis

The SEM images were imported into Photoshop® 7.0 (Adobe Systems, San Jose, CA) and xylem vessel lumina were selected and filled with white to facilitate the quantification of area. The image analysis program IP Lab version 3.6 (Scanalytics, Fairfax,VA) was calibrated using the SEM images of the carbon replica grating. The images were imported into IP Lab and the thickness of sclerenchyma and xylem cell walls and xylem luminal area were measured.

Preparation of cell wall samples

The midribs were isolated by removal of the leaf blade tissue, using the remainder of the leaves used for SEM sample preparation. The midribs were dried for 4 d in an oven set at 50 °C, ground in a Wiley mill to pass a 1 mm screen, and extracted in 50% (v/v) ethanol to remove soluble sugars and phenolics. The ear leaf of three independent plants per genotype was collected and used for the dissection of the sclerenchyma on the abaxial side of the midrib, as described by Vermerris *et al.* (2002). Stem tissue from three plants per genotype was collected at physiological maturity.

Histochemical reactions

Several pieces of dissected midribs were treated with acid phloroglucinol (Wiesner reagent) as described by Vermerris *et al.* (2002), and scanned on a flat-bed scanner. In order to investigate the origin of the brown colour in the mutants, midrib samples were incubated overnight in 6 ml 5:1 v/v DMSO:NH_4OH containing 1.7% (w/v) $NaBH_4$. This results in the reduction of aldehydes and ketones to their corresponding alcohols. The excess $NaBH_4$ was removed by adding 0.1 ml glacial acetic acid, followed by rinsing the samples twice in water and once in acetone. This protocol was based on procedures described by Tsai *et al.* (1998) and Carpita *et al.* (2001).

Pyrolysis-GC-MS

This technique relies on the thermal degradation of tissue samples under anoxic conditions. The pyrolysate contains volatile compounds that are separated by gas chromatography and identified with mass spectrometry. This method provides information on the composition of aromatic compounds in the cell wall. Information is also obtained on the composition of cell wall polysaccharides, but this information is limited because of degradation of the original compounds. A major advantage of Py-GC-MS is that it only requires small amounts of tissue (Boon, 1989; Ralph and Hatfield, 1991; Fontaine *et al.*, 2003). Like most analytical techniques that are used to analyse lignin composition, including thioacidolysis (Lapierre, 1993) and 'derivatization followed by reductive cleavage' (Lu and Ralph, 1997), Py-GC-MS provides compositional information on the fraction of the lignin in which the monomers are cross-linked via β-*O*-4 linkages (Lapierre, 1993), which represents the most common linkage in maize (Marita *et al.*, 2003). Py-GC-MS was performed as described by Bout and Vermerris (2003), using 1 mg samples of dissected midrib tissue. In order to evaluate the content of *p*-coumarate and ferulate, the midrib samples were *trans*-methylated as described by Vermerris and Boon (2001) and subjected to Py-GC-MS.

Klason lignin analysis

Klason lignin is defined as the ash-corrected residue remaining after the cell wall polysaccharides have been removed via acid hydrolysis. The procedure was based on the method described by Theander and Westerlund (1986), with the modifications of Hatfield *et al.* (1994). One hundred milligrams of ground midrib tissue or ground stem tissue that had been extracted in warm 50% (v/v) ethanol for 30 min was used for this analysis.

Cellulose determination

Cellulose content was determined as acetic-nitric acid resistant material obtained from 50 mg dried and ground midrib tissue, assayed spectrophotometrically using the anthrone reagent (Updegraff, 1969). α-Cellulose (SigmaAldrich, St Louis, MO) was used as a standard.

Statistical analyses

It was first determined whether height and peak area percentages in the pyrograms and cell wall characteristics showed evidence for differences between the wild type and the mutants. The following fixed effects model was used: $Y_{ij} = \mu + g_i + \varepsilon_{ij}$, where Y_{ij} is the peak area percentage or cell wall characteristic, the parameter μ is the overall mean, g_i the genotypic effect *i* from individual *j* and ε_{ij} the experimental error. To determine whether genotypes were statistically significantly different, pair-wise means were compared using Tukey's least significant difference at a threshold of 5% (Steel *et al.*, 1996). For those measurements that showed evidence of at least one pair-wise difference, the compounds were compared to each other using Pearson's correlation (Steel *et al.*, 1996).

In order to facilitate the visualization of differences among genotypes, the average peak area percentage was calculated across replicates. Averages were standardized for each peak area and a hierarchical clustering analysis was performed. In addition, a linear discriminant analysis (LDA) was performed to determine whether the four genotypes could be distinguished based on their chemical profiles. Compounds included in the LDA had to show statistically significant differences in at least one pair-wise comparison between genotypes. The statistical analyses were performed using SAS and JMP (SAS Institute, Cary, NC).

Results

Single bm *mutants and most double* bm *mutants are well within the normal range*

Single *bm* mutations have reported changes in flowering time (Vermerris and McIntyre, 1999; Vermerris *et al.*, 2002) and, in the case of *bm3*, increased susceptibility to *Fusarium* rot (Zuber *et al.*, 1977) and reduced yield (Gentinetta *et al.*, 1990). These mutants have been receiving interest as a potential source of lignocellulosic biomass for fuel production, as they can yield more fermentable sugars upon enzymatic saccharification compared to the same amount of biomass from a wild-type control (Vermerris *et al.*, 2007). Important for biomass production, the height differences in the single mutants compared with the wild type are modest (Fig. 1; see Supplementary Table S1 at *JXB* online). When independent *bm* mutations are combined, some phenotypic differences are identified. The height of the double mutants *bm1-bm2*, *bm3-bm4*, and *bm2-bm4* is statistically significantly different from the wild type (Fig. 1). Additional differences in height exist, such as between *bm1-bm2* and *bm2-bm3* (see Supplementary Table S1 at *JXB* online). All plants with the exception of *bm2-bm4*, however, flowered and set seed.

The bm2-bm4 *double mutant is radically different from wild type and the single mutants* bm2 *and* bm4

Figure 2 illustrates the drastically reduced height of a mature *bm2-bm4* mutant and its very dark brown midribs which, in contrast to the *bm2* and the *bm4* single mutants, are consistently visible from the adaxial side of the leaf. While the double mutant displayed in this image was viable and ultimately produced seed, the majority (>80%) of the *bm2-bm4* plants never reach maturity. Instead, their development is often arrested prior to or at the four-leaf stage. Observational evidence indicates that the size of the leaves and midribs tends to correlate with the height of the *bm2-bm4* plants. The *bm2-bm4* seed has been planted over a period of five years in different geographical regions in the United States (North Carolina, Indiana; summer) and in Puerto Rico (winter), and in different soils and in the greenhouse. Intense irrigation and application of fertilizer were of no avail. The *bm2-bm4* double mutant has been generated independently several times and displays a consistent phenotype, so that the developmental differences cannot be attributed to a parent with one or more additional spontaneous mutations, or to maternal effects during seed production. The two triple mutants that include *bm2* and *bm4*, namely *bm1-bm2-bm4* and *bm2-bm3-bm4* are unable to develop into mature plants under the conditions tested. Plants shown to be *bm1-bm2-bm4* triple mutants stopped growing at a very early seedling stage, wilted, and died (Fig. 2). Based on the inability to identify *bm2-bm3-bm4* seedlings among segregating progeny, the combination of those three mutations appears to arrest growth even prior to seedling emergence.

Why is bm2-bm4 *so different from the* bm2 *and* bm4 *single mutants and other double mutants?*

The brown colour of the vascular tissue in mutants or transgenics in which lignin biosynthesis was compromised has been attributed to the accumulation of coniferaldehyde (Higuchi *et al.*, 1994; Mackay *et al.*, 1997; Tsai *et al.*, 1998; Vermerris *et al.*, 2002). The lignin of the *bm1* mutant is indeed known to accumulate high levels of coniferaldehyde end-groups (Halpin *et al.*, 1998; Vermerris *et al.*, 2002). To test the hypothesis that coniferaldehyde is responsible for the brown colour of the midribs in *bm* mutants other than

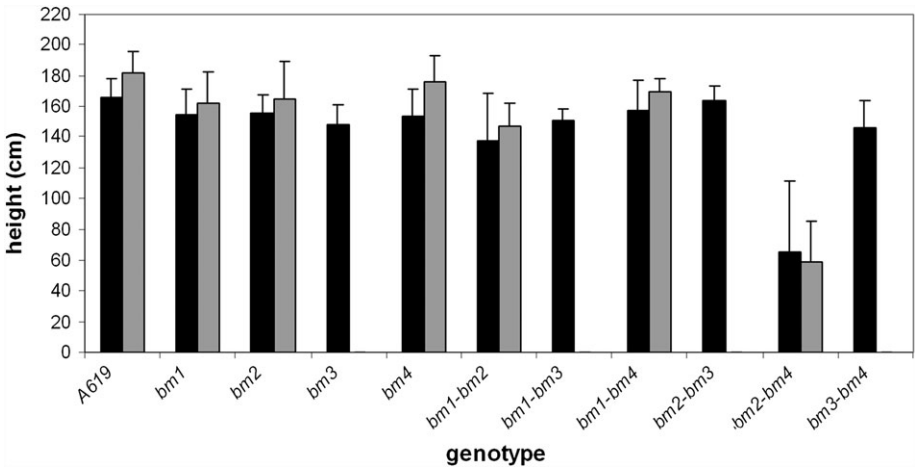

Fig. 1. Height at anthesis of wild-type inbred A619 and near-isogenic single and double *bm* mutants in two consecutive years (Year 1, grey bars; Year 2, black bars). Not all double mutants were available in the first year. Error bars indicate 1 SD.

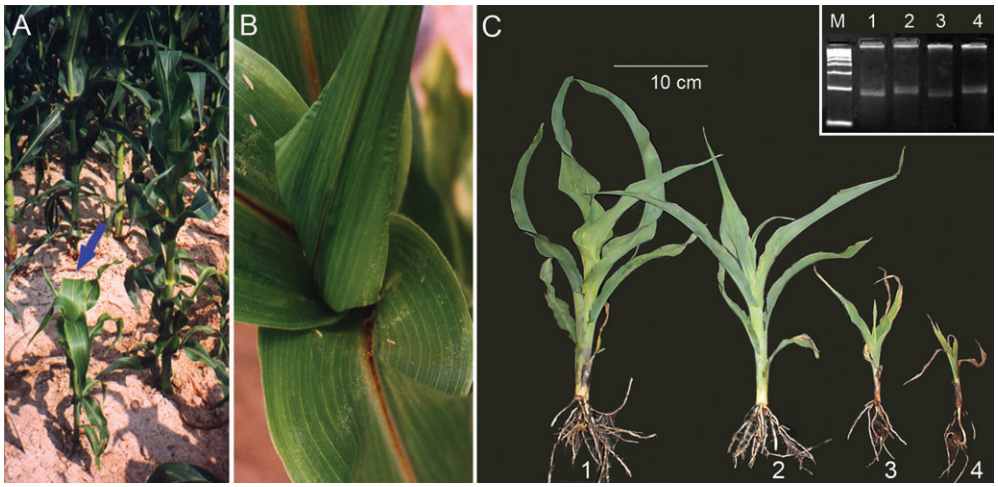

Fig. 2. (A) The *bm2-bm4* double mutant (blue arrow) is significantly shorter and thinner than the single mutants *bm2* (shown to the right) and *bm4*. (B) The vascular tissue of the *bm2-bm4* mutant is dark-brown. (C) Six-week old, field-grown seedlings of inbred A619 (1) and near-isogenic mutants *bm1-bm2* (2), *bm2-bm4* (3), and *bm1-bm2-bm4* (4). Inset: Gel image showing the PCR product obtained with SSR marker dupSSR10. Numbers correspond to image 1C. M is a 100 bp ladder.

bm1, dissected midribs from the mutants *bm2*, *bm4*, and *bm2-bm4* were stained with acid phloroglucinol, with wild-type and *bm1* midribs as controls. The unstained *bm2-bm4* midribs are the darkest, followed by the *bm2*, *bm4*, and *bm1* midribs (Fig. 3). After staining with phloroglucinol the *bm1* midribs produce the expected, intense staining, whereas the *bm4*, *bm2*, and *bm2-bm4* samples display much less coloration, indicating that they contain fewer rather than more coniferaldehyde end-groups. If the brown colour in the vascular tissue of the *bm* mutants is the result of the accumulation of aldehydes and/or ketones, as suggested by Tsai *et al.* (1998), reduction with $NaBH_4$ would be expected to eliminate the brown colour. Figure 3 shows that the $NaBH_4$ treatment results in a yellowing of the wild-type and *bm1* midribs after the complete reduction of the coniferaldehyde-end groups. The reduction with $NaBH_4$ lessens but does not completely eliminate the brown colour of *bm2*, *bm4*, and *bm2-bm4* midribs, indicating a different chemical origin of the brown color in these mutants compared to *bm1* plants.

To characterize the phenotype of the *bm2*, *bm4* and *bm2-bm4* mutants further, Klason lignin content in the leaf midribs and mature stem sections was determined (Table 1). The effect of these mutations on Klason lignin content in the mature stems is small and not statistically significant and confirms the limited effect of *bm2* and *bm4* on stem tissue harvested prior to flowering time reported by Marita *et al.* (2003). In contrast, in the midribs the *bm2* and *bm4* mutations, each cause an 11% reduction in Klason lignin content, and this effect is additive in the *bm2-bm4* mutant.

Since the Klason lignin indicated that the *bm2* and *bm4* mutations primarily affect the leaves, the cell wall composition of the wild-type, *bm2*, *bm4*, and *bm2-bm4* samples was analysed in more detail using pyrolysis-GC-MS. The average peak areas of a set of diagnostic compounds were identified from the different cell wall constituents (Table 2). The pyrograms do not contain evidence for the appearance

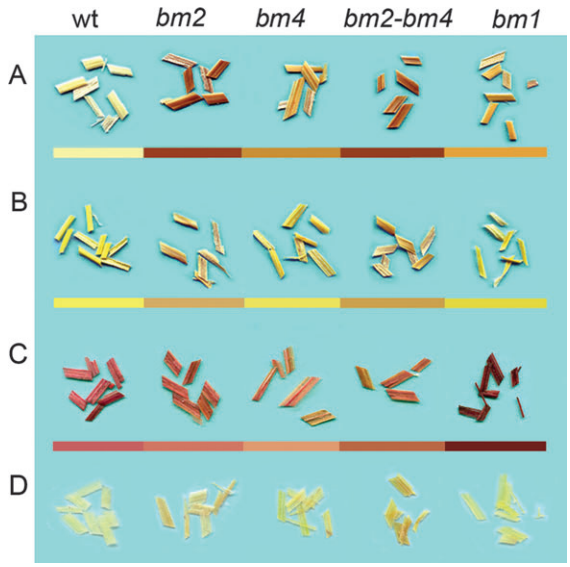

Fig. 3. Colour differences between dissected vascular tissue of the *brown midrib* mutants. (A) Dissected vascular bundles of inbred A619 and the near-isogenic *brown midrib* mutants *bm1* (on far right), *bm2*, *bm4*, and *bm2-bm4*. The samples were prepared from leaf 6 at anthesis. (B) The same samples as in (A) after $NaBH_4$ reduction. (C) The same samples as in (A) after reaction with acid phloroglucinol. (D) The same samples as in (B) after reaction with acid phloroglucinol. The coloured bars underneath each sample represent the predominant colour based on the average of a representative 5×5-pixel area.

of novel residues that could be associated with the brown colour of the vascular tissue. The compound 3-(4-hydroxyphenyl)-3-oxopropanal, derived from H-residues, was not detected in all samples, making statistical comparisons invalid. This compound was, therefore, not considered in further analyses. The remaining compounds were tested for pairwise differences (Table 3). Many compounds derived

Table 1. Klason lignin content (mean and standard deviation) of midribs and stems from leaf 6 of wild-type, *bm2*, *bm4*, and *bm2-bm4* plants

* indicates $P<0.05$, ** indicates $P<0.01$, and *** indicates $P<0.001$ for a pair-wise difference in Klason lignin content of midrib tissue after correcting for multiple comparisons. For stem tissue, there were no statistically significant differences.

Genotype	Different from	Klason lignin (g g^{-1} DW)			
		Midrib		Stem	
		Mean	SD	Mean	SD
Wild type	*bm2***,*bm4***,*bm2-bm4****	0.166	0.008	0.23	0.03
bm2	*wt***,*bm2-bm4**	0.146	0.003	0.21	0.01
bm4	wt**,*bm2-bm4***	0.149	0.000	0.20	0.01
bm2-bm4	*wt***,*bm2**,*bm4***	0.130	0.002	0.21	0.02

Table 2. Chemical composition of dissected midribs from leaf 6 of wild-type, *bm2*, *bm4* and *bm2-bm4* plants obtained with Py-GC-MS

The name of the compounds, their origin (PS, polysaccharides, H, *p*-hydroxyphenyl residue; G, guaiacyl residue; S, syringyl residue; FA, ferulate; pCA, *p*-coumarate), and their respective mean peak area percentages (obtained after integrating the pyrograms from three midrib samples per genotype) are listed. The cellulose content (mg g^{-1}) was determined based on the anthrone assay.

	Compound	Origin	Peak area percentage			
			wt	*bm2*	*bm4*	*bm2-bm4*
1	Furfural	PS	2.77	3.30	3.22	3.43
2	2,3-dihydro-5-methylfuran-2-one	PS	2.79	3.11	3.20	2.99
3	(5H)-furan-2-one	PS	1.63	1.83	1.88	1.83
4	4-hydroxy-5,6-dihydro-(2H) pyran-2-one	PS	0.82	1.61	1.46	1.85
5	4-ethylphenol	H	1.01	1.03	0.92	1.07
6	4-methylguaiacol	G	0.93	0.57	0.55	0.48
7	4-vinyl phenol	pCA/H	8.73	7.42	5.74	7.17
8	4-vinyl guaiacol	FA/G	6.24	4.48	4.12	3.52
9	2,6-dimethoxyphenol	S	1.56	0.80	0.93	0.90
10	3-(4-hydroxyphenyl)-3-oxopropanal	H	0.29	0.34	0.48	0.55
11	2,6-dimethoxy-4-vinyl-phenol	S	0.64	0.46	0.35	0.44
12	Coniferyl aldehyde	G	0.87	0.36	0.37	0.25
13	Coniferyl alcohol	G	0.87	0.27	0.35	0.23
14	Acetosyringone	S	0.66	0.29	0.45	0.27
	Cellulose		501	519	496	503

from lignin are reduced in the *bm2*, *bm4*, and *bm2-bm4* mutants compared with the wild type, whereas compounds corresponding to breakdown products from cell wall carbohydrates are increased in intensity. The midribs of both the *bm2* and *bm4* mutants show overall similar and statistically significant reductions in compounds derived from guaiacyl and syringyl residues in the lignin (Table 3). There are no statistically significantly different differences between *bm2* and *bm2-bm4*, whereas *bm4* and *bm2-bm4* are different in both coniferaldehyde and acetosyringone, indicating that the composition of the *bm2-bm4* double mutant is more similar to the *bm2* mutant than the *bm4* mutant (Fig. 4). The compounds 4-vinylphenol and 4-vinylguaiacol are abundant pyrolysis products that can be derived from both lignin (H and G residues, respectively) and hydroxycinnamic acids (*p*-coumarate and ferulate, respectively). Based on the pyrograms, only the midribs of the *bm4* mutant showed a reduction in 4-vinylphenol, 35% less than the wild type. By contrast, the levels of 4-vinylguaiacol were reduced in the *bm2* and *bm4* mutants, and dramatically further in the *bm2-bm4* double mutant. *Trans*-methylated midrib samples were analysed with Py-GC-MS in order to determine to what extent these changes were attributable to changes in the levels of hydroxycinnamic acids. This indicated that both the *bm4* and the *bm2-bm4* samples contained 30% less (of the dimethyl ester of) *p*-coumarate than the wild type, whereas the *bm2* sample did not differ from the wild type. These data are consistent with the increase in H-derived compounds observed in the *bm2-bm4* mutant. The level of (the dimethyl ester of) ferulate was reduced by 10, 30, and 40% in the *bm2*, *bm4*, and *bm2-bm4* mutants, respectively, which largely explains the reductions in 4-vinylguaiacol.

Given the considerable pyrolytic degradation of fragments derived from cell wall carbohydrates, cellulose content was determined via wet chemical analysis. No significant variation in cellulose content was observed among the different genotypes (Table 2). Given the decrease in Klason lignin and the increase in pentose-derived pyrolysis fragments, the cell walls of the mutants must contain more hemicellulosic polysaccharides that compensate for the reduction in lignin.

The similarities in chemical changes in the *bm2* and *bm4* single mutants as determined by Py-GC-MS, and the apparent additive effects on Klason lignin could be the result of both mutations affecting the same metabolic or developmental process(es) independently. If *Bm2* and *Bm4* act sequentially in a linear process, the double mutant would reflect the phenotype associated with a mutation in the upstream gene. The score plot resulting from a linear discriminant analysis of the pyrolysis data (Fig. 5) shows that all four genotypes can be clearly separated from each other based on the chemical composition of their midribs. This suggests that *Bm2* and *Bm4* have different functions that are not part of a linear pathway or process.

Does variation in cell wall composition translate into ultrastructural variation?

Scanning electron microscopy was performed to determine how the observed changes in cell wall composition affected the ultrastructure of the cell walls in the vascular tissue of the midrib. Figure 6 shows representative cross-sections of the midrib in the different genotypes. The most striking difference can be observed in the sclerenchyma, which is the supportive tissue between the xylem and the epidermis. The walls of the sclerenchyma cells are much thicker in the mutants, particularly in the double mutant, compared to the

Table 3. *P*-values for pair-wise comparisons among genotypes for chemical composition

P- values listed are corrected for multiple comparisons using Tukey's LSD.

Compound	*wt* versus *bm2*	*wt* versus *bm4*	*wt* versus *bm2-bm4*	*bm2* versus *bm4*	*bm2* versus *bm2-bm4*	*bm4* versus *bm2-bm4*
Furfural	0.0481	0.0934	0.0161	0.9636	0.8539	0.6060
2,3-dihydro-5-methylfuran-2-one	0.3037	0.1394	0.6399	0.9344	0.9004	0.6061
(5H)-furan-2-one	0.1591	0.0741	0.1591	0.9451	1.0000	0.9451
4-hydroxy-5,6-dihydro-(2H) pyran-2-one	0.0198	0.0528	0.0043	0.8910	0.6513	0.3019
4-ethylphenol	0.9996	0.8991	0.9694	0.8590	0.9850	0.6831
4-metylguaiacol	0.0010	0.0007	0.0002	0.9750	0.3811	0.5916
4-vinylphenol	0.2862	0.0098	0.1780	0.1405	0.9830	0.2289
4-vinylguaiacol	0.0032	0.0010	0.0002	0.7216	0.0800	0.3358
2,6-dimethoxyphenol	0.0042	0.0128	0.0098	0.8109	0.8985	0.9969
2,6-dimethoxy-4-vinyl-phenol	0.0614	0.0054	0.0381	0.3349	0.9855	0.4946
Coniferylaldehyde	0.0000	0.0000	0.0000	0.9929	0.0655	0.0450
Coniferylalcohol	0.0000	0.0000	0.0000	0.6393	0.9490	0.3657
Acetosyringone	0.0001	0.0040	0.0000	0.0162	0.9334	0.0075

wild type. Higher magnification (×1000) images clearly show that the secondary wall no longer adheres to the primary wall. While this could be a result of the sectioning as opposed to being reflective of the *in vivo* situation, it does indicate that the physical characteristics of the sclerenchyma in the double mutant are very different from those of the wild type. A quantitative analysis was performed to assess variation in cell wall thickness between the different genotypes. The results of this analysis are shown in Table 4. This table does not include the double mutant because, due to the loss of adherence, it was not possible to make accurate measurements of wall thickness. It is apparent that the cell walls of the *bm2* and *bm4* mutant are statistically significantly different (P <0.001), and, on average, 2.3 and 1.8 times, respectively, thicker than the wild-type sclerenchyma walls.

Changes in the size of the xylem vessels were evaluated by measuring individual xylem vessel area in cross-sections from the different genotypes (Table 4). The area of xylem vessels in the *bm2* mutant was smaller, but not statistically significantly different from the wild-type xylem vessels. The area of the xylem vessels in the *bm4* mutant was significantly larger. By contrast, the *bm2-bm4* double mutant had xylem vessels that were significantly smaller than the wild type and the two single mutants. In addition, a 'stringy' material can be observed on the cut surface of the vascular tissue in the double mutant. The chemical nature of this material is unknown, but its appearance may be a result of the chemical differences described above.

Discussion

Defining the relationship between the structure and function of complex polymers is important in understanding the chemical basis for physical properties. This can provide insights into how species evolved and diverged, and is of help in attempts to improve field performance of crop plants (resistance to biotic and abiotic stress), and to tailor the composition of biological materials to enhance downstream applications through the use of genetic modification (Chen and Dixon, 2007; Vermerris *et al.*, 2007; Saballos *et al.*, 2008).

The Klason lignin and pyrolysis analyses indicate that the *bm2* and *bm4* mutations primarily affect the cell wall composition of the leaves, as opposed to the stems and thus act in a tissue-specific manner. This explains why the chemical composition of the stalks of these two mutants was similar to that of the wild-type control, in sharp contrast to what was observed for the *bm1* and *bm3* mutants (Marita *et al.*, 2003; Barrière *et al.*, 2004). The leaf-specific effects of the *bm2* and *bm4* mutations also explain why the yield of fermentable sugars obtained from enzymatic saccharification of *bm2* and *bm4* stover, which is composed primarily of stem tissue, was not significantly different from that of wild-type stover (Vermerris *et al.*, 2007), and why there is no brown coloration in the vascular tissue of the stem.

The SEM images reveal significant changes in ultrastructure in both the xylem and the sclerenchyma cells, with the increase in cell-wall thickness of the sclerenchyma in all three mutants being unexpected. A number of mutants and transgenic plants in which lignin biosynthetic genes were down-regulated had very thin secondary walls that could not withstand the negative pressure in the xylem. Consequently, the xylem cells collapsed (Piquemal *et al.*, 1998; Jones *et al.*, 2001; Franke *et al.*, 2002; Day *et al.*, 2009). Down-regulation of both the *cinnamyl alcohol dehydrogenase* (*CAD*) and *cinnamoyl-CoA reductase* (*CCR*) genes in tobacco resulted in thinner and more irregular xylem walls (Chabannes *et al.*, 2001), and mutations in the sorghum genes encoding cinnamyl alcohol dehydrogenase2 (Saballos *et al.*, 2009; Sattler *et al.*, 2009) and caffeic acid *O*-methyltransferase (Bout and Vermerris, 2003) were shown to result in thinner sclerenchyma cell walls (Palmer *et al.*, 2008). The difference between these studies and the data reported here could be the result of differences between species, the impact of changes in gene expression on specific

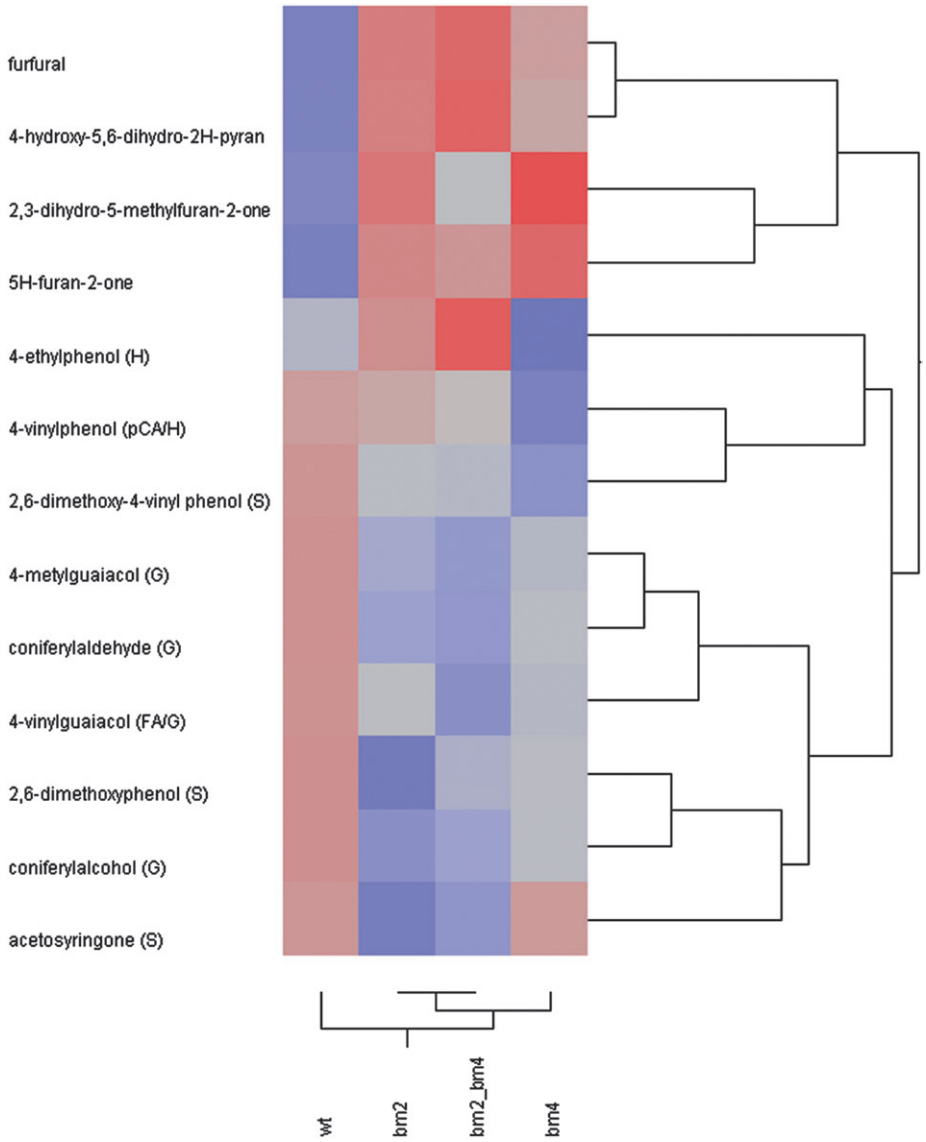

Fig. 4. For each genotype the average value of the measured chemical composition was calculated. Each compound's average across genotypes was subtracted from the genotypic mean to centre the data. A heatmap based on a hierarchical cluster analysis performed on the average peak area percentage across replicates is depicted, where blue indicates lower levels of the compound relative to the overall average and red indicates higher levels of the compound relative to the overall average. Only compounds for which there was a statistically significant difference observed are depicted.

tissues (e.g. sclerenchyma versus xylem vessels), or specific changes in cell wall composition.

There are several possible explanations for the increased cell wall thickness in the sclerenchyma. One possibility is that the reduction in lignin content has caused the cell walls to be more water-permeable. The cell wall carbohydrates, which are hydrophilic in nature, may have swollen as a result of the absorption of water. The lack of adherence of the cell walls may also be a result of the swelling. This effect may be enhanced by the apparent increase in the content of hemicellulosic polysaccharides. Alternatively, the reduction in ferulic acid levels in the walls of the mutants may reduce the degree of crosslinking between lignin and glucuronoarabinoxylans, resulting in a less compact wall structure that is not as well adhered to the primary wall.

The increase in the content of hemicellulosic polysaccharides may reflect the existence of a compensatory mechanism that the plant activates in response to a reduction in lignin content or certain changes in lignin composition. The presence of compensatory mechanisms was proposed by Hu *et al.* (1999) based on observations of poplar plants in which lignin content had been reduced as a result of down-regulation of the *4-coumarate-CoA ligase* (*4CL*) gene. In these plants the reduction in lignin content resulted in a concomitant increase in cellulose content. Furthermore, the rice *brittle culm1* mutant, which has reduced cellulose content, was shown to contain more lignin based on staining with phloroglucinol and Klason lignin determination (Li *et al.*, 2003). Similar observations were reported for the maize *brittle stalk2* mutant (Ching *et al.*, 2006; Sindhu

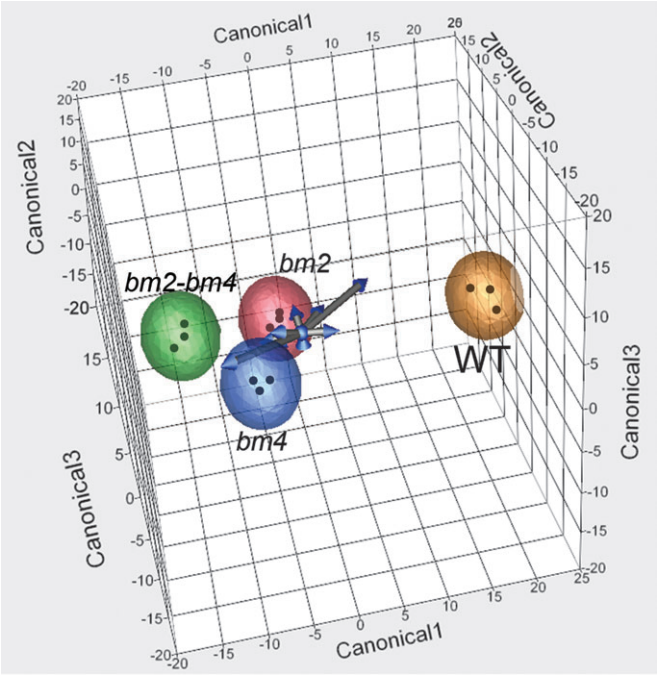

Fig. 5. Discriminant function score plot displaying the different genotypes based on the chemical composition of the cell wall based on Py-GC-MS. Canonical 1 explains 83% of the variance; Canonical 2 explains 12% of the variance. The dark dots represent the three replicates per genotype.

et al., 2007). The latter study also provided evidence for an increase in GAX in response to a reduction in cellulose. These studies, combined with the results presented here, provide evidence for an interdependence between the different cell wall polymers.

The altered structure of the midrib in the *bm* mutants is likely to impact the function of the conducting tissues in terms of both water and mineral transport. The drought symptoms and reduced growth of the *bm2-bm4* mutant is probably the result of the reduced diameter of the xylem vessels, which not only limits the flux, but also requires a higher pressure to transport xylem sap. The reduced hydrophobicity as a result of the lower lignin content further exacerbates these effects, as hydraulic properties of xylem tissue are influenced by the degree of lignification and mineral content of the xylem sap (Zwieniecki *et al.*, 2001; Boyce *et al.*, 2004). By extrapolation, the changes in xylem vessel structure in the *bm1-bm2-bm4* mutant may be even more extreme, thereby completely preventing normal growth. An additional factor that may play a role is variation in torsion resulting from torque applied by the wind. Thin-walled hollow tubes experience less torsion than a solid cylinder of the same dimensions. The thin-walled sclerenchyma cells of the wild type may experience less torsion than the thick-walled sclerenchyma cells of the *bm2-bm4* mutant. Increased torsion in the double mutant may stress or damage adjoining cells, hence compromising cell function and ultimately growth and development. These hypotheses warrant further investigations by follow-up

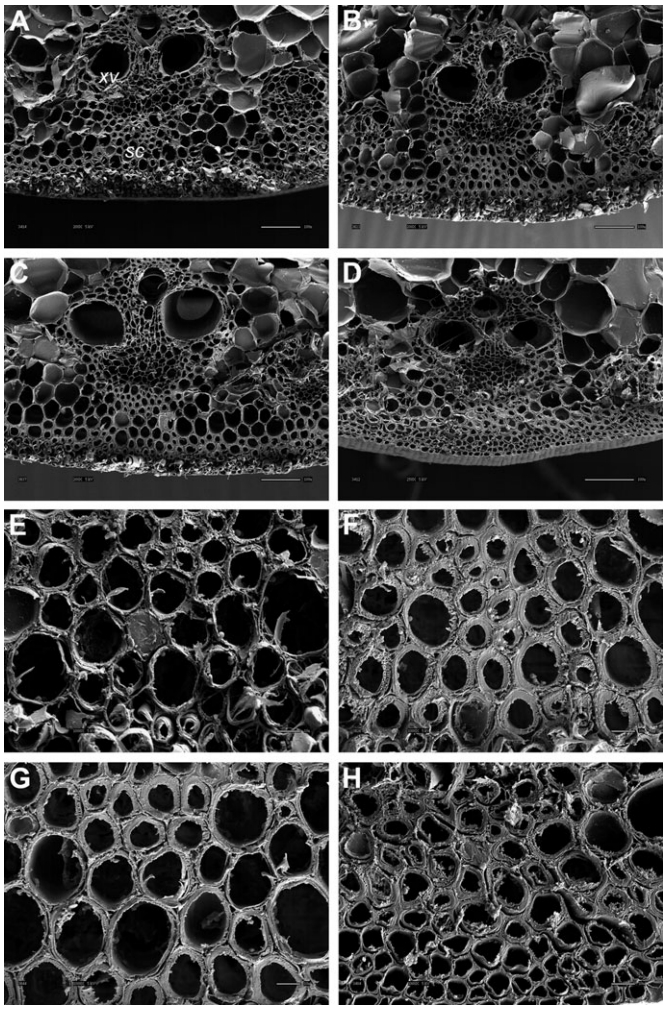

Fig. 6. SEM images of cross sections through the midrib. (A, E) Wild type, (B, F) *bm2*, (C, G) *bm4*, and (D, H) *bm2-bm4*. (A–D) represent overview images, whereas (E–H) represent close-up views of the sclerenchyma. The magnification in images (A–C) is ×200, in (D) ×250, and in (E–F) ×1000. The white bars represent 100 μm and 10 μm in images (A–D) and (E–F), respectively. SC, sclerenchyma; XV, xylem vessel.

Table 4. Cell wall thickness of sclerenchyma cells and surface area of the xylem vessels (mean and standard deviation) measured in SEM images from wild-type, *bm2*, *bm4*, and *bm2-bm4* plants

The means of the cell wall thickness are based on 25–50 measurements per SEM image from three samples per genotype, and did not include the *bm2-bm4* mutant. The means of the xylem vessel area are based on two xylem vessels for each of three tissue samples per genotype. * indicates P <0.05, ** indicates P <0.01, and *** indicates P <0.001 for a pair-wise difference after correcting for multiple comparisons with Tukey's LSD.

Genotype	Different from	Wall thickness (μm)		Different from	Area (μm²)	
		Mean	SD		Mean	SD
Wild type	*bm4****	0.244	0.089	*bm4****,*bm2-bm4****	6911	893
bm2	*bm4****	0.575	0.122	*bm4***,*bm2-bm4****	6013	452
bm4	wt***,*bm2****	0.447	0.077	wt***,*bm2***,*bm2-bm4****	9892	917
bm2-bm4		na	na	wt***,*bm2****,*bm4****	3899	828

biophysical studies, ideally in a way that also allows separation of effects of the mutations on the sclerenchyma versus xylem vessels.

Based on the combined data presented here, it is apparent that variation in cell wall composition affects the physical parameters of the secondary cell walls in sclerenchyma tissue, with reductions in G- and S-content and a concomitant increase in hemicellulosic polysaccharides leading to thicker walls. The changes in chemical composition of the *bm2-bm4* double mutant, which may be a result of fundamental changes in gene expression regulation (Guillaumie *et al.*, 2007), are severe enough to compromise growth and development. The addition of the *bm1* mutation to create a triple mutant *bm1-bm2-bm4* resulted in a genotype in which this limit was apparently exceeded as evidenced by the failure to develop to a point where tissue could be sampled for chemical analysis. Given that all of the other *bm* double mutants and the triple mutants that do not contain *bm2* and *bm4* are appreciably more vigorous, these observations demonstrate that there is a limit to the metabolic plasticity of cell wall composition which should be taken into consideration when engineering plants for down-stream processing.

Supplementary data

Supplementary data can be found at *JXB* online.

Supplementary Table S1. Height measurements in the wild type (inbred A619) and all single and double *bm* mutants.

Acknowledgements

The authors thank William Foster and Phil Devillez for excellent assistance in the field, Javier Campos and Stephany Esposito for assistance with the lignin analyses, and Drs Nicholas Carpita, Michael Ladisch, and Paul Sisco for their support. Part of this research was supported by The Consortium for Plant Biotechnology Research, Inc. by DOE Prime Agreement No. DEFG36-02GO12026 (to WV). This support does not constitute an endorsement by DOE or by The Consortium for Plant Biotechnology Research, Inc. of the views expressed in this publication. Additional financial support from the National Science Foundation Plant Genome Research Project 0821954 (to LMM), the Showalter Foundation, Dow AgroSciences, and the University of Florida is gratefully acknowledged.

References

Barrière Y, Ralph J, Méchin V, Guillaumie S, Grabber JH, Argillier O, Chabbert B, Lapierre C. 2004. Genetic and molecular basis of grass cell wall biosynthesis and degradability. II. Lessons from brown midrib mutants. *Comptes Rendus Biologies* **327,** 847–860.

Bicerano J. 2002. *Prediction of polymer properties*. New York: Marcel Dekker.

Boerjan W, Ralph J, Baucher M. 2003. Lignin biosynthesis. *Annual Review of Plant Biology* **54,** 519–546.

Boon JJ. 1989. An introduction to pyrolysis mass spectrometry of lignocellulosic material: case studies of barley straw, corn stem and *Agropyron*. In: Chesson A, Ørskov ER, eds. *Physico-chemical characterisation of plant residues for industrial and feed use*. London: Elsevier Applied Science, 25–49.

Bout S, Vermerris W. 2003. A candidate gene-approach to clone the sorghum *Brown midrib* gene encoding caffeic acid *O*-methyltransferase. *Molecular Genetics and Genomics* **269,** 205–214.

Boyce CK, Zwieniecki MA, Cody GD, Jacobsen C, Wirick S, Knoll AH, Holbrook NM. 2004. Evolution of xylem lignification and hydrogel transport regulation. *Proceedings of the National Academy of Sciences, USA* **101,** 17555–17558.

Carpita NC, Defernez M, Findlay K, Wells B, Shoue DA, Catchpole G, Wilson RH, McCann MC. 2001. Cell wall architecture of the elongating maize coleoptile. *Plant Physiology* **127,** 551–565.

Carpita NC, Gibeaut DM. 1993. Structural models of the primary cell walls in flowering plants: consistency of molecular structure with the physical properties of the wall during growth. *The Plant Journal* **3,** 1–30.

Chabannes M, Ruel K, Yoshinaga A, Chabbert B, Jauneau A, Joseleau J-P, Boudet A- M. 2001. *In situ* analysis of lignins in transgenic tobacco revelas a differential impact of individual transformations on the spatial patterns of lignin deposition at the cellular and subcellular levels. *The Plant Journal* **28,** 271–282.

Chabbert B, Tollier MT, Monties B. 1994*a*. Biological variability in lignification of maize: expression of the brown midrib bm3 mutation in three maize cultivars. *Journal of the Science of Food and Agriculture* **64,** 349–355.

Chabbert B, Tollier MT, Monties B, Barrière Y, Argillier O. 1994*b*. Biological variability in lignification of maize: expression of the brown midrib bm2 mutation. *Journal of the Science of Food and Agriculture* **64,** 455–460.

Chen F, Dixon RA. 2007. Lignin modification improves fermentable sugar yields for biofuel production. *Nature Biotechnology* **25,** 759–761.

Ching A, Dhugga KS, Appenzeller L, Meeley R, Bourett TM, Howard RJ, Rafalski A. 2006. *Brittle stalk2* encodes a putative glycosylphosphatidylinositol-anchored protein that affects mechanical strength of maize tissues by altering the composition and structure of secondary cell walls. *Planta* **224,** 1174–1184.

Davin BL, Lewis NG. 2005. Lignin primary structures and dirigent sites. *Current Opinion in Biotechnology* **16,** 407–415.

Davin LB, Jourdes M, Patten AM, Kim K-W, Vassão DG, Lewis NG. 2008. Dissection of lignin macromolecular configuration and assembly: comparison to related biochemical processes in allyl/propenyl phenol and lignan biosynthesis. *Natural Product Reports* **25,** 1015–1090.

Day A, Neutelings G, Nolin F, *et al*. 2009. Caffeoyl coenzyme A *O*-methyltransferase down-regulation is associated with modifications in lignin and cell-wall architecture in flax secondary xylem. *Plant Physiology and Biochemistry* **47,** 9–19.

Fontaine AS, Bout S, Barrière Y, Vermerris W. 2003. Variation in cell wall composition among forage maize (*Zea mays* L.) inbred lines

and its impact on digestibility: Analysis of neutral detergent fiber composition by pyrolysis-gas chromatography-mass spectrometry. *Journal of Agriculture and Food Chemistry* **51,** 8080–8087.

Franke R, Humphreys JM, Hemm MR, Denault JW, Ruegger MO, Cusumano JC, Chapple C. 2002. The Arabidopsis *REF8* gene encodes the 3-hydroxylase of phenylpropanoid metabolism. *The Plant Journal* **30,** 33–45.

Gentinetta E, Bertolini M, Rossi I, Lorenzoni C, Motto M. 1990. Effect of brown midrib-3 mutant on forage quality and yield in maize. *Journal of Genetics and Breeding* **44,** 21–26.

Groth D, Santini J, Hamaker B, Weil C. 2008. High-throughput screening of EMS mutagenized maize for altered starch digestibility. *Bioenergy Research* **1,** 118–135.

Guillaumie S, Pichon M, Martinant JP, Bosio M, Goffner D, Barrière Y. 2007. Differential expression of phenylpropanoid and related genes in *brown-midrib bm1, bm2, bm3*, and *bm4* young near-isogenic maize plants. *Planta* **226,** 235–250.

Halpin C, Holt K, Chojecki J, Oliver D, Chabbert B, Monties B, Edwards K, Barakate A, Foxon GA. 1998. *Brown-midrib* maize (*bm1*): a mutation affecting the cinnamyl alcohol dehydrogenase gene. *The Plant Journal* **14,** 545–553.

Hatfield R, Vermerris W. 2001. Lignin formation in plants: the dilemma of linkage specificity. *Plant Physiology* **126,** 1351–1357.

Hatfield RD, Jung HG, Ralph J, Buxton DR, Weimer PJ. 1994. A comparison of the insoluble residues produced by the Klason lignin and acid detergent lignin procedures. *Journal of the Science of Food and Agriculture* **65,** 51–58.

Hatfield RD, Ralph J, Grabber JH. 1998. Cell wall cross-linking by ferulates and diferulates in grasses. *Journal of the Science of Food and Agriculture* **79,** 403–407.

Higuchi T, Ito T, Umezawa T, Hibino T, Shibata D. 1994. Red-brown color of lignified tissues of transgenic plants with antisense CAD gene: wine-red lignin from coniferaldehyde. *Journal of Biotechnology* **37,** 151–158.

Hu W-J, Harding SA, Lung J, Popko JL, Ralph J, Stokke DD, Tsai C-J, Chiang VL. 1999. Repression of lignin biosynthesis promotes cellulose accumulation and growth in transgenic trees. *Nature Biotechnology* **17,** 808–812.

Jones L, Ennos AR, Turner SR. 2001. Cloning and characterization of *irregular xylem4* (*irx4*): a severley lignin-deficient mutant of Arabidopsis. *The Plant Journal* **26,** 205–216.

Joseleau J-P, Ruel K. 1997. Study of lignification by noninvasive techniques in growing maize internodes. *Plant Physiology* **114,** 1123–1133.

Kortstee AJ, Suurs LCJM, Vermeesch AMG, Keetels CJAM, Jacobsen E, Visser RGF. 1998. The influence of an increasing degree of branching on the physico-chemical properties of starch from genetically modified potato. *Carbohydrate Policy* **37,** 173–184.

Lapierre C, Tollier MT, Monties B. 1988. Mise en évidence d'un nouveau type d'unité constitutive dans les lignines d'un mutant de maïs *bm3. Comptes Rendus de l'Académie des sciences Paris*, Serie III **307,** 723–728.

Lapierre C. 1993. Application of new methods for the investigation of lignin structure. In: Jung HG, Buxton DR, Hatfield RD, Ralph J, eds. *Forage cell wall structure and digestibility*. Madison, WI: ASA, CSCA, SSSA, 133–166.

Li Y, Qian Q, Zhou Y, *et al*. 2003. *BRITTLE CULM1*, which encodes a Cobra-like protein, affects the mechanical properties of rice plants. *The Plant Cell* **15,** 2020–2031.

Lu F, Ralph J. 1997. Derivatization followed by reductive cleavage (DFRC method), a new method for lignin analysis: protocol for analysis of DFRC monomers. *Journal of Agricultural and Food Chemistry* **45,** 2590–2592.

MacKay JJ, O'Malley DM, Presnell T, Booker F, Campbell MM, Whetten RW, Sederoff RR. 1997. Inheritance, gene expression, and lignin characterization in a mutant pine deficient in cinnamyl alcohol dehydrogenase. *Proceedings of the National Academy of Sciences, USA* **94,** 8255–8260.

Marita J, Vermerris W, Ralph J, Hatfield RD. 2003. Variations in the cell wall composition of maize *brown midrib* mutants. *Journal of Agricultural and Food Chemistry* **51,** 1313–1321.

Morrow SL, Mascia P, Self KA, Altschuler M. 1997. Molecular characterization of a brown midrib3 deletion mutant in maize. *Molecular Breeding* **3,** 351–357.

Müsel G, Schindler T, Bergfeld R, Ruel K, Jacquet G, Lapierre C, Speth V, Schopfer P. 1997. Structure and distribution of lignin in primary and secondary cell walls of maize coleoptiles analysed by chemical and immunological probes. *Planta* **201,** 146–159.

Nakashima J, Chen F, Jackson L, Shadle G, Dixon RA. 2008. Multi-site genetic modification of monolignol biosynthesis in alfalfa (*Medicago sativa*): effects on lignin composition in specific cell types. *New Phytologist* **179,** 738–750.

Palmer NA, Sattler SE, Saathoff AJ, Funnell D, Pedersen JF, Sarath G. 2008. Genetic background impacts soluble and cell wall-bound aromatics in *brown midrib* mutants of sorghum. *Planta* **229,** 115–127.

Piquemal J, Lapierre C, Myton K, O'Connell A, Schuch W, Grima-Pettenati J, Boudet AM. 1998. Down-regulation of cinnamoyl-CoA reductase induces significant changes of lignin profiles in transgenic tobacco plants. *The Plant Journal* **13,** 71–83.

Ralph J, Grabber JG, Hatfield RD. 1995. Lignin–ferulate cross-links in grasses: active incorporation of ferulate polysaccharide esters into ryegrass lignins. *Carbohydrate Research* **275,** 167–178.

Ralph J, Hatfield RD. 1991. Pyrolysis-GC-MS characterization of forage materials. *Journal of Agricultural and Food Chemistry* **39,** 1426–1437.

Ralph J, Lundquist K, Brunow G, *et al*. 2004. Lignins: natural polymers from oxidative coupling of 4-hydroxyphenylpropanoids. *Phytochemistry Review* **3,** 29–60.

Saballos A, Ejeta G, Sanchez E, Kang CH, Vermerris W. 2009. A genomewide analysis of the cinnamyl alcohol dehydrogenase family in sorghum [*Sorghum bicolor* (L.) Moench] identifies *SbCAD2* as the *Brown midrib6* gene. *Genetics* **181,** 783–795.

Saballos A, Vermerris W, Rivera L, Ejeta G. 2008. Allelic association, chemical characterization and saccharification properties of *brown midrib* mutants of sorghum (*Sorghum bicolor* (L.) Moench). *Bioenergy Research* **1,** 193–204.

Sattler S, Saathoff AJ, Palmer NA, Funnell-Harris DL, Sarath G, Pedersen JF. 2009. A nonsense mutation in a cinnamyl alcohol dehydrogenase gene is responsible for the sorghum *brown midrib 6* phenotype. *Plant Physiology* **150,** 584–595.

Sindhu A, Langewisch T, Olek A, Multani DS, McCann MC, Vermerris W, Carpita NC, Johal G. 2007. Maize *Brittle stalk2* encodes a COBRA-like protein expressed in early organ development but required for tissue flexibility at maturity. *Plant Physiology* **145,** 1444–1459.

Steel RGD, Torrie JH, Dickey DA. 1996. *Principles and procedures of statistics: a biometrical approach*. New York, NY: McGraw Hill.

Terashima N, Fukushima K, He L-F, Takabe K. 1993. Comprehensive model of the lignified plant cell wall. In: Jung HG, Buxton DR, Hatfield RD, Ralph J, eds. *Forage cell wall structure and digestibility*. Madison, WI: ASA-CSSA-SSSA, 247–270.

Theander O, Westerlund EA. 1986. Studies on dietary fiber. 3. Improved procedures for analysis of dietary fiber. *Journal of Agricultural and Food Chemistry* **34,** 330–336.

Tsai C-J, Popko J, Mielke MR, Hu W-J, Podila GK, Chiang VL. 1998. Suppression of *O*-methyltransferase gene by homologous sense transgene in quaking aspen causes red-brown wood phenotypes. *Plant Physiology* **117,** 101–112.

Updegraff D. 1969. Semi-micro determination of cellulose in biological materials. *Analytical Biochemistry* **32,** 420–424.

Vanholme R, Morreel K, Ralph J, Boerjan W. 2008. Lignin engineering. *Current Opinion in Plant Biology* **11,** 278–285.

Vermerris W, Boon JJ. 2001. Tissue-specific patterns of lignification are disturbed in the *brown midrib2* mutant of maize (*Zea mays* L.). *Journal of Agricultural and Food Chemistry* **49,** 721–728.

Vermerris W, McIntyre LM. 1999. Time to flowering in *brown midrib* mutants of maize: an alternative approach to the analysis of developmental traits. *Heredity* **83,** 171–178.

Vermerris W, Saballos A, Ejeta G, Mosier NS, Ladisch MR, Carpita NC. 2007. Molecular breeding to enhance ethanol production from corn and sorghum stover. *Crop Science* **47,** S145–S153.

Vermerris W, Thompson KJ, McIntyre LM. 2002. The maize *Brown midrib1* locus affects cell wall composition and plant development in a dose-dependent manner. *Heredity* **88,** 450–457.

Vignols F, Rigau J, Torres MA, Capellades M, Puigdomènech P. 1995. The *brown-midrib3* (*bm3*) mutation in maize occurs in the gene encoding caffeic acid *O*-methyl transferase. *The Plant Cell* **7,** 407–416.

Willats WGT, Orfial C, Limberg G, *et al*. 2001. Modulation of the degree and pattern of methyl-esterification of pectic homogalacturonan in plant cell walls. *Journal of Biological Chemistry* **276,** 19404–19413.

Yang B, Wyman CE. 2004. Effect of xylan and lignin removal by batch and flowthrough pretreatment on the enzymatic digestibility of corn stover cellulose. *Biotechnology and Bioengineering* **86,** 88–95.

Zhang A, Lu F, Sun R, Ralph J. 2009. Ferulate-coniferyl alcohol cross-coupled products formed by radical coupling reactions. *Planta* **229,** 1099–1108.

Zuber MS, Colbert TR, Bauman LF. 1977. Effect of *brown-midrib-3* mutant in maize (*Zea mays* L.) on stalk strength. *Zeitschrift für Pflanzenzüchtung* **79,** 310–314.

Zwieniecki MA, Melcher PJ, Holbrook NM. 2001. Hydrogel control of xylem hydraulic resistance in plants. *Science* **291,** 1060–1062.